THE ASTROPHYSICAL JOURNAL, 520:L135–L138, 1999 August 1

PLASMA DIAGNOSTICS OF TRANSITION REGION "MOSS" USING *SOHO*/CDS AND *TRACE*

LYNDSAY FLETCHER[1] AND BART DE PONTIEU[1,2]

Received 1999 March 29; accepted 1999 June 2; published 1999 June 28

ABSTRACT

Recent observations of solar active regions with the *Transition Region and Coronal Explorer* (*TRACE*) have revealed finely textured, low-lying EUV emission, called the "moss," appearing as a bright dynamic pattern with dark inclusions. The moss has been interpreted as the upper transition region by Berger and coworkers. In this study we use *SOHO* Coronal Diagnostic Spectrometer and *TRACE* observations of Active Region 8227 on 1998 May 30 to determine the physical parameters of the moss material. We establish that the plasma responsible for the moss emission has a temperature range of (0.6–1.5) × 10^6 K and is associated with hot loops ($T > 2 \times 10^6$ K). Moss plasma has an electron density of (2–5) × 10^9 cm^{-3} at a temperature of 1.3 × 10^6 K, giving a pressure of 0.7–1.7 dynes cm^{-2} (a few times higher than in coronal loops observed in the *TRACE* Fe IX/X λ171 passband). The volume filling factor of the moss plasma is of order 0.1, and the path along which the emission originates is of order 1000 km long.

Subject headings: Sun: chromosphere — Sun: corona — Sun: transition region

1. INTRODUCTION

Recent high-resolution observations with the *Transition Region and Coronal Explorer* (*TRACE*) instrument (Handy et al. 1999) have revealed a new type of emission, known as the "moss." It is a finely textured, low-lying bright emission, most prominently seen in the Fe IX/X λ171 bandpass of *TRACE*. A good example of a patch of moss is shown in Figure 1*e* around (−350″, 370″). Morphological and dynamical aspects of this active region (AR) emission are described by Berger et al. (1999), who conclude that the moss is emission from the upper transition region. The known properties of the moss described in that paper are the large-scale moss pattern, consisting of patches on scales of 20,000–30,000 km, which occurs over plage (AR magnetic network), but only in the vicinity of hot loops. The moss base is at a mean height of 2800 ± 600 km above the photosphere with an apparent vertical extent at the solar limb of 1000–3000 km. The mossy texture, formed by bright emission and dark inclusions, is structured on scales of 2000–3000 km and varies rapidly on timescales of a minute. The variation is partly intrinsic, partly due to variation in extinction by the dark inclusions, which correlate closely with dark jets in chromospheric Hα ± 350 mÅ images. Based on their observations, Berger et al. (1999) advance the idea that the *TRACE* moss emission is due to heating of low-lying plasma by thermal conduction from overlying hot loops. Similar low-lying emission, most likely the same phenomenon, was observed at low resolution with the Normal Incidence X-Ray Telescope (NIXT; Peres, Reale, & Golub 1994).

To determine the physical parameters of the moss plasma, we employ simultaneous *TRACE* and *SOHO* Coronal Diagnostic Spectrometer (CDS; Harrison et al. 1995) observations of NOAA Active Region 8227 (N26°.7, E10°.4). We use CDS data taken on 1998 May 30 with the Normal Incidence Spectrometer (NIS). The AR_MON raster with an area of 240″ × 240″ and a pixel size of 4″.0 × 3″.4 was made between 06:33:03 and 07:28:57 UTC and contains 20 spectral windows. A second raster made between 10:30:06 and 11:27:31 UTC has the full NIS spectral range and images a narrow strip (20″ × 240″) with pixel size 2″.0 × 1″.7. The CDS data were calibrated using W. Thompson's calibration of 1998 December 23.[3] The higher resolution (pixel size 0″.5) *TRACE* images are used to clearly identify moss and other features in the CDS images.

In this Letter we examine the appearance of the AR in spectral lines formed between 10^5 and 2.5 × 10^6 K, and we obtain the differential emission measure (DEM) of moss plasma (§ 2). In addition, we determine the density of moss plasma at 10^6, 1.3 × 10^6, and 1.6 × 10^6 K (§ 3). In § 4 we discuss whether models of the moss are consistent with our measured physical parameters and set limits on the filling factor and the emission length scale of the moss.

2. TEMPERATURE OF MOSS PLASMA

The moss is most easily visible in the *TRACE* 171 Å bandpass, predicted to be dominated by lines from Fe IX and Fe X with temperatures of maximum (equilibrium) ionization fractions, T_{max}, of ~10^6 K. However, because of the low formation height of the moss and its close association with plage, it was initially suggested that moss emission could be from lower temperature transition region lines in this bandpass, e.g., the O VI λ173 lines with $T_{max} = 3 \times 10^5$ K. We address this by examining the CDS O V λ629.7 spectroheliogram (Fig. 1*b*), which has $T_{max} = 2.5 \times 10^5$ K, close to that of the O VI lines. The O V spectroheliogram does not show good correspondence with the *TRACE* 171 Å image (Fig. 1*e*). Most O V emission occurs above plage, whereas *TRACE* 171 Å moss emission occurs above some, but not all, of the plage visible in O V. For example, the patch of plage visible in O V around (−270″, 510″) does not show up in the *TRACE* 171 Å image. If the moss were O VI emission, we would expect all plage visible in O V to appear at the same relative strength in the *TRACE* 171 Å image. That it does not suggests strongly that the moss is not low-temperature contamination of the *TRACE* 171 Å passband.

CDS rasters made simultaneously in lines of increasing T_{max}

[1] Lockheed Martin Solar and Astrophysics Laboratory, Department L9-41, Building 252, 3251 Hanover Street, Palo Alto, CA 94304; fletcher@lmsal.com, bdp@lmsal.com.

[2] Max-Planck-Institut für extraterrestrische Physik, Giessenbachstrasse, D-85740 Garching bei München, Germany.

[3] W. Thompson, 1998 CDS-SOFT mailing list (see http://orpheus.nascom.nasa.gov/cds/cds_soft_index.html).

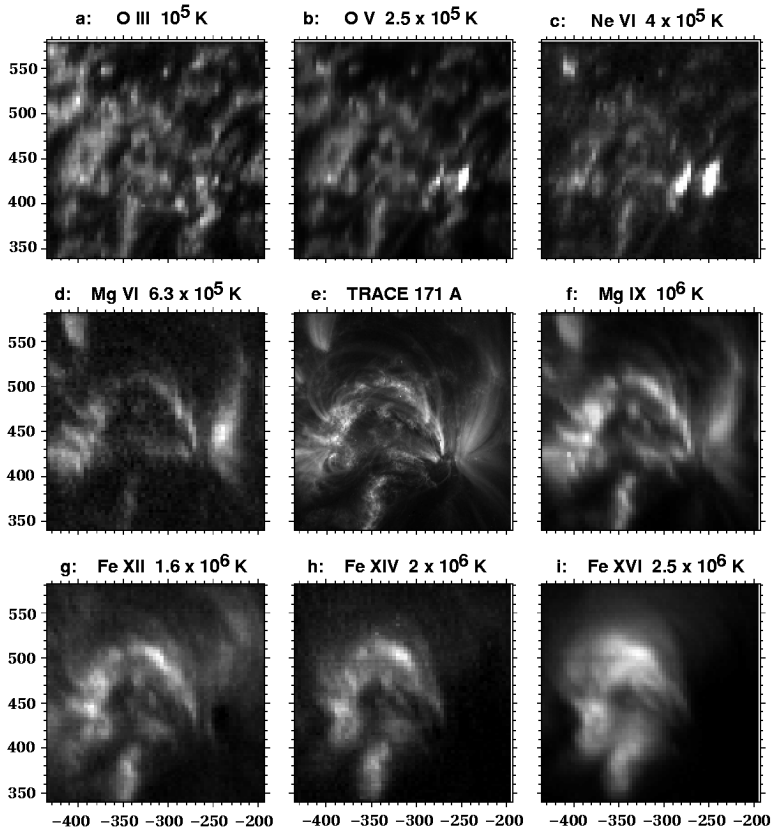

FIG. 1.—(*a–d*, *f–i*) Spectroheliograms of AR 8227 at the line center of eight lines from the AR_MON raster taken with CDS between 06:33:03 and 07:28:57 UTC on 1998 May 30, and the corresponding *TRACE* 171 Å image (*e*) taken at 07:10:58 UTC. The Mg IX line (*f*) is close to a Mg VII line ($T_{\max} = 6.3 \times 10^5$ K) at 367.7 Å, which we have removed by fitting two components to the spectral profile. The finely textured emission known as "moss" is clearly visible in the *TRACE* image, e.g., around (−350″, 370″). The CDS spectroheliograms show how the large-scale moss pattern is identifiable between 0.6×10^6 and 1.6×10^6 K. The (*x*, *y*)-axes are in arcseconds. North is up, and east is to the left.

(Fig. 1) show how the large-scale moss pattern (consisting of many moss patches clearly identifiable in the *TRACE* 171 Å image, Fig. 1*e*) emerges with increasing temperature. At low temperatures (e.g., O III at 1.6×10^5 K) all plage has approximately the same intensity. With increasing temperature a subset of the plage becomes more enhanced. It corresponds to the *TRACE* 171 Å large-scale moss pattern. This pattern becomes distinct from the rest of the plage for $T_{\max} \sim (0.6\text{–}1.6) \times 10^6$ K. At yet higher temperatures diffuse loop structures become visible, possibly joining patches of moss. Moss is seen only where both plage and Fe XVI ($T_{\max} = 2.5 \times 10^6$ K) loops are present. This supports the finding of Berger et al. (1999) that moss occurs in the vicinity of high-temperature loops. The CDS Mg IX λ368.1 spectroheliogram with $T_{\max} = 10^6$ K (Fig. 1*f*) shows the best correspondence with the *TRACE* 171 Å image (Fig. 1*e*). Both mossy regions and coronal loops are visible, at about the same relative intensity down to a scale of a few CDS pixels. This suggests that most of the *TRACE* 171 Å emission originates from plasma at 10^6 K.

This qualitative picture of the temperature dependence of moss emission is confirmed quantitatively by a DEM analysis. By calculating the DEM $\phi(T) \equiv N_e^2 (dh/dT)$, we can determine $\phi(T)dT$, which is a measure of the amount of material along the line of sight in the temperature interval T to $T + dT$. Using the CHIANTI package (Dere et al. 1987), we derive $\phi(T)$ for a 6″ × 22″ patch of moss around (−350″, 370″) from the intensities of 20 spectral lines in the full NIS spectral range. We have assumed constant pressure of $n_e T = 5 \times 10^{15}$ cm^{-3} K (see § 4) and coronal abundances of Meyer (1985) with lowered (by a factor of 1.5) Mg and Si abundances. This adjustment is made to ensure consistency of DEM values from different elements at identical temperatures. Note that the Si and Mg abundance values of Waljeski et al. (1994) (higher by an order of magnitude) result in a very poor fit of the DEM and are thus not applicable to our AR. The resulting DEM, shown in Figure 2, confirms that along the line of sight there is more plasma at temperatures of $(0.8\text{–}1.6) \times 10^6$ K than there is at $(2\text{–}4) \times 10^5$ K. We have thus established that the moss seen in the *TRACE* 171 Å passband is dominated by emission from million-degree plasma.

3. ELECTRON DENSITY OF MOSS PLASMA

An average electron density of the moss plasma can be obtained from density-sensitive line ratio diagnostics in the CDS spectral range. To apply the diagnostic, one must assume that both lines are from the same emitting volume, which is at the $T_{\max}$ for the ion under study. The method is thus independent of filling factors. However, the density obtained is an emissivity-weighted average over the resolving element and will be biased toward the higher end of the range of densities which is undoubtedly present (Almleaky, Brown, & Sweet 1989).

We apply the Si X diagnostic ($T_{\max} = 1.3 \times 10^6$ K) to the AR_MON raster. In each pixel the Si X lines at 347.3 Å and the blend at 356.05, 356.012 Å are fitted with Gaussians and

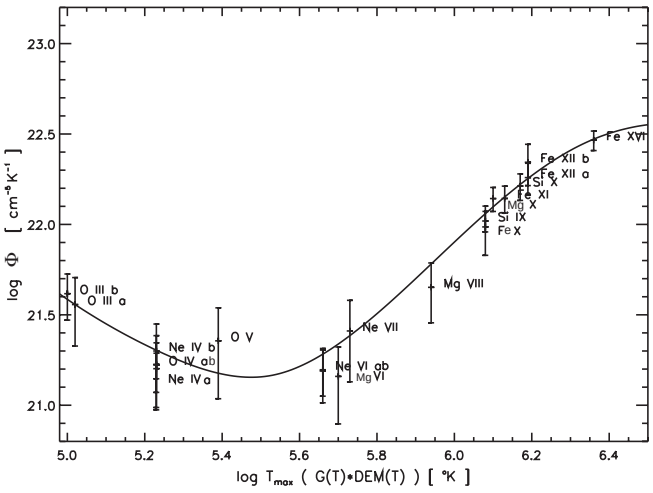

FIG. 2.—The results of a DEM analysis carried out on a small patch of moss around (−350″, 370″) in AR 8227 on 1998 May 30 using the full CDS/NIS spectral range. The intensities of the following lines were used: O III λ525.8, O III λ599.6, Ne IV λ542.1, Ne IV λ544.0, O IV λ554.5, O IV λ555.3, O V λ629.7, Ne VI λ558.6, Ne VI λ562.8, Mg VI λ349.1, Ne VII λ561.6, Mg VIII λ339.0, Si IX λ349.8, Fe X λ345.7, Mg X λ624.9, Fe XI λ341.1, Si X λ347.4, Fe XII λ346.8, Fe XII λ364.5, and Fe XVI λ360.8. The error bars on each symbol represent the uncertainties associated with the intensity measurements only.

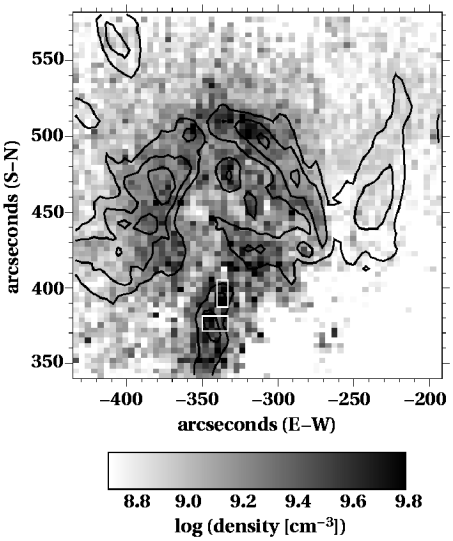

FIG. 3.—Density map of AR 8227 made using the Si X λλ347.4, 356.0 density diagnostic. Black contours are of Mg IX λ368.1 intensity. The small white rectangles indicate approximate locations where further diagnostics from the full-spectrum NIS raster have been applied. In the white region in the lower right-hand corner, counts are too low to determine densities. See text for details.

a constant background, and the intensity ratios are mapped to density values using the CHIANTI software. The resulting density map is shown in Figure 3, overlaid by contours of the Mg IX λ368.1 emission (see Fig. 1*f*). The density in moss regions is significantly higher than that in the loops. Furthermore, there are density variations between different moss regions, and it is noteworthy that those free of bright *TRACE* 171 Å loops [e.g., around (−350″, 370″)] have a higher density than those with *TRACE* 171 Å loops ending in them [e.g., (−390″, 440″)]. The typical density n_e for the moss at a temperature of 1.3×10^6 K is $(2–5) \times 10^9$ cm^{-3}; *TRACE* loops at the same temperature have $n_e \sim (0.8–1.2) \times 10^9$ cm^{-3}.

Other density diagnostics from lines in the CDS raster covering the full NIS spectral range are applied on the moss region around (−350″, 370″). We binned intensities in small areas (marked in Fig. 3) and derived a mean density value. The error estimates on the densities are based on the influence of photon statistics on the intensities in a single pixel. The values in Table 1 confirm that moss plasma typically has a density of $(2–7) \times 10^9$ cm^{-3}. Such a spread of values at very similar temperatures is to be expected when using line ratio diagnostics on inhomogeneous plasmas, as Almleaky et al. (1989) demonstrated.

4. DISCUSSION AND CONCLUSIONS

Our observations show that the large-scale *TRACE* 171 Å moss pattern is identifiable in spectral lines of ions formed between 6×10^5 and 1.6×10^6 K. Our DEM analysis confirms the predominance of million-degree plasma in moss regions. Like Berger et al. (1999), we find that moss occurs only in plage associated with hot ($>2 \times 10^6$K) loops, typically invisible or only partially visible in the *TRACE* 171 Å passband. With densities of $(2–5) \times 10^9$ cm^{-3} at $T = 1.3 \times 10^6$ K, the plasma pressure in the moss $p_m \sim 0.7–1.7$ dynes cm^{-2} (assuming fully ionized hydrogen with $T_e = T_i$). This is about 3 times the pressure in *TRACE* loops at the same temperature, which are rarely associated with moss. Our data thus support the conclusion of Berger et al. (1999) that moss emission originates from *million-degree* plasma of the upper transition region of hot loops, with an elevated pressure, connecting with plage. The typical "mossy" texture is due to the presence, at the same height, of million-degree, EUV-emitting plasma and jets of dense, chromospheric plasma.

The mossy texture visible in *TRACE* 171 Å images implies that moss emission in 1 CDS pixel has a maximum value $f_{A,\max}$ of the area filling factor f_A of 0.3–0.5. This is considerably higher than most reported values for f_A in the *lower* transition region which fall in the range 10^{-5}–10^{-2} (Mariska 1992, p. 176). The thickness of the moss at the limb is of order a few thousand kilometers (Berger et al. 1999). This provides us with an upper limit $\Delta L_{\max}$ of the emission integration length ΔL. Despite its lower spatial resolution, we can use CDS to form an independent estimate of the product $f_V \Delta L$ for the moss, in which f_V is the volume filling factor. Given that $f_V \le f_A$, we can thus obtain a better fix on f_V or ΔL separately. We use equation (9) in Brosius et al. (1996) to obtain

$$f_V \Delta L = \frac{I}{0.8 n_e^2 A_b C}, \qquad (1)$$

with the usual assumption that $n_{\rm H} = 0.8 n_e$. The intensity of the spectral line is I, n_e is the electron density at $T_{\max}$ (determined

TABLE 1

AVERAGE ELECTRON DENSITY n_e IN TWO MOSS REGIONS USING CDS DIAGNOSTICS AND THE PRODUCT OF VOLUME FILLING FACTOR f_V AND EMISSION INTEGRATION LENGTH ΔL FOR REGION 2

Ion	$T_{\max}$ (10^6 K)	n_e(Moss 1) (10^9 cm^{-3})	n_e(Moss 2) (10^9 cm^{-3})	$f\Delta L$ (km)
Si IX	1.0	>1.7	>3.5	1000–5000
Si X	1.3	$2.1^{+1.1}_{-0.7}$	$3.2^{+4.0}_{-1.4}$	1000–4000
Fe XII	1.6	>5.3	$4.2^{+1.4}_{-1.0}$	2000–6000

independently from line pair diagnostics), A_b is the element abundance, and C is the contribution function (from the CHIANTI database). Taking into account the range of possible and probable values for n_e, I, and A_b, we determine $f_V \Delta L$ (listed in the last column of Table 1) for Si IX λ349.8, Si X λ347.4, and Fe XII λ346.8. These are consistent with one another and indicate that $f\Delta L$ is of order 2000 km, for abundances similar to those used in our DEM analysis. We also know from the above that $f_V \Delta L < f_{V,\max} \Delta L_{\max} \leq f_{A,\max} \Delta L_{\max} \sim 1000$ km. This strongly suggests that the volume filling factor of the moss f_V is not much below the value of the area filling factor $f_{A,\max}$ seen with *TRACE*. Additionally, the thickness of the moss as seen from above (i.e., almost at disk center) is probably at least about 1000 km. This provides a minimum thickness of the upper transition region (i.e., $0.6 \times 10^6 < T < 1.6 \times 10^6$ K) above plage. Note that the higher abundances reported by, e.g., Waljeski et al. (1994) would result in values of $f_V \Delta L$ an order of magnitude lower. However, as argued in § 2, we believe these higher abundances are not applicable to the moss in our AR.

Berger et al. (1999) conclude that the moss emission originates in a classical transition region (CTR)—the interface between hot (million degree) coronal loops and a cool chromosphere. Our work supports this conclusion. A contrasting view advocates that most of the TR emission originates in unresolved fine structure (UFS), i.e., small loops of a few hundred thousand degrees, thermally isolated from the corona (Feldman 1983; Dowdy, Emslie, & Moore 1987). Dowdy et al. (1987) reject the CTR view, finding it impossible to reconcile the slope and magnitude of the quiet-Sun DEM with CTR models in any reasonable flux tube geometry. We cannot reject the CTR view on this basis. Our DEM curve is substantially different from that of Dowdy et al. (1987), and their quiet-Sun models do not apply to the moss. The CTR case is strengthened by Martens & Kankelborg (1999), who show that whereas a UFS model *cannot*, a CTR model *can* provide the moss emission measure observed by *TRACE*.

The slope of our DEM as a function of temperature is substantially higher than typical quiet-Sun values, which are about 0.8 in a plot of $\log \phi$–$\log T$. In Figure 3 we find a slope of 1.8 ± 0.3 for $5.5 < \log T < 6.2$, very similar to what Brosius et al. (1996) find for two ARs (1.8 and 2.0, respectively). Steeper slopes such as this can be explained not only by expanding flux tubes but also by the presence of flows (Athay 1981; Mariska 1992, p. 212).

We find that the pressure in moss plasma is higher than in *TRACE* loops at the same temperature. This is qualitatively consistent with the results of loop modeling undertaken by Peres et al. (1994) to explain apparently low-lying, high-temperature emission observed with the NIXT (probably unresolved moss emission). They concluded that in "high"-pressure loops, EUV emission occurs low down, where the million-degree temperature range of the CTR is squeezed into the lowest parts of the loop. The moss pressure we obtain falls within the range (0.1–30 dynes cm^{-2}) Peres et al. (1994) considered, but very much at the lower end. Our data thus imply that loops having a relatively modest, although elevated, pressure can cause moss emission. Their model predicts that at a pressure of 1 dyne cm^{-2} a 10-fold decrease in emission along the loop occurs over a distance of about 10^4 km. However, both limb observations by Berger et al. (1999) and our determination of ΔL indicate that this distance is of order 1000 km and possibly shorter. This discrepancy may be due to the dependence of the model of Peres et al. (1994) on the temperature response curve of NIXT, which is more sensitive at higher temperatures than *TRACE* in the 171 Å passband and thus images more plasma along the loop. It would be useful to repeat the analysis of Peres et al. (1994) for the *TRACE* temperature response curve using our densities and temperatures and including, e.g., flows and dynamic changes, in line with *TRACE* observations (Schrijver et al. 1999). Preliminary analysis of Doppler shifts of CDS spectral lines CDS indicate that the moss does not show very fast (>20 km s^{-1}) up- or downflows.

Note that much of our analysis is based on the assumption of ionization equilibrium. Departures from this equilibrium can introduce errors in estimates of temperature and density of the plasma. In particular, in the presence of flows, low densities and rapid cooling or heating can lead to a departure of the local electron temperature from the value $T_{\max}$ expected in ionization equilibrium. While we defer a full discussion to a future paper, CHIANTI calculations confirm that, e.g., our Si X density measurements are rather robust with respect to such departures from ionization equilibrium.

To conclude, the combination of the diagnostic power of CDS and the high resolution of *TRACE* have allowed us to study the moss emission in detail. This and future moss studies will lead to an improved understanding of the structure, energetics, and dynamics of the upper transition region in ARs.

We are grateful to the CDS and *TRACE* teams for building and operating their instruments and providing software, to R. Harrison and A. Fludra for making available the CDS data, and to C. J. Schrijver, C. Kankelborg, and T. E. Berger for helpful discussions. *SOHO* is a project of international cooperation between ESA and NASA.

REFERENCES

Almleaky, Y. M., Brown, J. C., & Sweet, P. A. 1989, A&A, 224, 328
Athay, R. G. 1981, ApJ, 249, 340
Berger, T. E., De Pontieu, B., Schrijver, C. J., & Title, A. M. 1999, ApJ, 519, L97
Brosius, J. W., Davilla, J. M., Thomas, R. J., & Monsignori-Fossi, B. C. 1996, ApJS, 106, 143
Dere, K. P., Landi, E., Mason, H. E., Monsignori-Fossi, B. C., & Young, P. R. 1997, A&AS, 125, 149
Dowdy, J. F., Jr., Emslie, A. G., & Moore, R. L. 1987, Sol. Phys., 112, 255
Feldman, U. 1983, ApJ, 275, 367
Handy, B. N. et al. 1999, Sol. Phys., in press
Harrison, R. A. et al. 1995, Sol. Phys., 162, 233
Mariska, J. T. 1992, The Solar Transition Region (Cambridge: Cambridge Univ. Press).
Martens, P. C. H., & Kankelborg, C. C. 1999, ApJ, submitted
Meyer, J. P. 1985, ApJS, 57, 173
Peres, G., Reale, F. & Golub, L. 1994, ApJ, 422, 412
Schrijver, C. J., et al. 1999, Sol. Phys., in press
Waljeski, K. et al. 1994, ApJ, 429, 909